GMR
The Original

ANTI-INFLAMMATORY ACTIVITY OF ULTRASOUND-MEDIATED GREEN SYNTHESIS OF CUO NANOPARTICLES USING *ECTOCARPALES* (MARINE MACROALGAE) EXTRACT AND THEIR INTEGRATION INTO STARCH/PVA ELECTROSPUN NANOFIBERS

Vasundhara Chandirasekar[1], Anoosh Golla[2], Narasimhalu CRV[3], Alagendran Subbarayalu[4], Kaliyamoorthy Dass[5*]

[1]Saveetha Medical College & Hospital (SMCH), Saveetha Institute of Medical and Technical Sciences (SIMATS), Thandalam, Chennai, Tamil Nadu 602105, India. Email: vasudevichandra@gmail.com
[2]Department of Neurology, Saveetha Medical College and Hospital, Saveetha Institute of Medical And Technical Sciences (SIMATS), Thandalam, Chennai-602105, Tamil Nadu, India. Email: anushyadav2025@gmail.com.
[3]Department of Dermatology, Saveetha Medical College and Hospital, Saveetha Institute of Medical And Technical Sciences (SIMATS), Thandalam, Chennai-602105, Tamil Nadu, India. Email: narasimhalucrv.smc@saveetha.com; ORCID: https://orcid.org/0009-0005-8261-5512
[4]Saveetha College of Nursing (SCON), Saveetha Institute of Medical and Technical Sciences (SIMATS), Chennai – 602105, Tamil Nadu, India. Email: alagendrans.scon@saveetha.com; ORCID: https://orcid.org/0009-0009-0749-7180
[5*]Natural Product and Vector Control Research Lab, Department of Pharmacology, Saveetha Medical College and Hospital, Saveetha Institute of Medical And Technical Sciences (SIMATS), Thandalam, Chennai-602105, Tamil Nadu, India. Email: dass.smc@saveetha.com; ORCID: https://orcid.org/0000-0002-4564-3275

ABSTRACT

This study presents the green synthesis, characterization, and anti-inflammatory evaluation of copper oxide (CuO) nanoparticles (NPs) derived from *Ectocarpales* extract and their incorporation into starch/polyvinyl alcohol (PVA) nanoscaffolds. UV–Visible spectroscopy confirmed the distinct optical features of both the algal extract and CuO NPs. Fourier-transform infrared spectroscopy (FT-IR) and X-ray Diffraction (XRD) analyses verified the formation and structural integration of CuO NPs within the polymeric matrix. Scanning Electron Microscopy (SEM) imaging revealed uniform nanoparticle dispersion within nanofibers exhibiting desirable porosity, while Thermogravimetric Analysis (TGA) indicated enhanced thermal stability. Dynamic light scattering (DLS) and zeta potential measurements demonstrated moderate nanoparticle stability and positive surface charge. Anti-inflammatory activity, evaluated via protein denaturation and xanthine oxidase inhibition assays, showed concentration-dependent efficacy, with nanoscaffolds displaying superior inhibition compared to CuO NPs and algal extract alone. These findings highlight the potential of starch/PVA/CuO-NP nanoscaffolds as effective, eco-friendly anti-inflammatory agents suitable for biomedical applications such as wound healing and tissue regeneration.

KEYWORDS: *Ectocarpales*, Green synthesis, CuO nanoparticles, Starch/PVA/CuO-NPs nanoscaffolds, Anti-inflammatory activity.

1. INTRODUCTION

The advancement of nanotechnology has significantly revolutionized the fields of material science and biomedical engineering, particularly in the development of novel functional materials with enhanced physicochemical and biological properties [1]. Among the various types of engineered nanomaterials, metal oxide nanoparticles have garnered considerable attention due to their exceptional surface-to-volume ratio, electronic configuration, and unique interactions with biological systems [2]. Specifically, copper oxide nanoparticles (CuO NPs) have emerged as promising candidates for biomedical applications, including antimicrobial, antioxidant, and anti-inflammatory therapies, owing to their low cost, abundance, catalytic efficiency, and intrinsic bioactivity [3]. However, conventional synthesis routes for CuO NPs often rely on harsh chemicals and energy-intensive methods, raising concerns about environmental safety and cytotoxicity [4]. Green synthesis has surfaced as an eco-friendly alternative to traditional chemical and physical methods, emphasizing the use of natural biological systems such as plant extracts, bacteria, fungi, and algae for nanoparticle production [5]. This approach capitalizes on the reducing, capping, and stabilizing abilities of naturally occurring phytochemicals, which facilitate the formation of nanoparticles under mild conditions [6]. Marine algae, particularly brown algae of the order *Ectocarpales*, are rich in a diverse array of bioactive compounds including phenolics, flavonoids, terpenoids, and polysaccharides [7]. These phytoconstituents not only assist in nanoparticle synthesis but may also impart synergistic therapeutic properties to the resulting nanomaterials [8]. The current study utilizes *Ectocarpales* algae, collected from the Rameswaram coastal region of Tamil Nadu, as a sustainable and renewable biological resource for the green synthesis of CuO NPs [9].

The biomedical significance of CuO NPs synthesized via green methods lies in their multifunctionality [10]. Several studies have demonstrated their broad-spectrum antimicrobial activity and ability to mitigate oxidative stress and

inflammation—key pathological features of chronic wounds and inflammatory disorders [11]. Nonetheless, the potential toxicity of free nanoparticles, their uncontrolled release, and poor biocompatibility remain major hurdles in clinical translation. Therefore, integrating these nanoparticles into biopolymeric matrices offers a promising strategy to improve their stability, bioavailability, and safety profile [12]. Electrospinning, a versatile and scalable technique for fabricating nanofibrous scaffolds, provides a unique platform for such integration [13]. Electrospun fibers exhibit high surface area-to-volume ratios, excellent porosity, and tunable mechanical properties, making them ideal for biomedical applications such as wound dressings, drug delivery systems, and tissue engineering scaffolds [14].

Among the biopolymers employed in electrospinning, starch and polyvinyl alcohol (PVA) stand out due to their biodegradability, biocompatibility, and film-forming abilities [15]. Starch, a natural polysaccharide obtained from agricultural sources, has a long history of safe use in pharmaceutical and biomedical fields [16]. However, its mechanical properties and processability are often limited [17]. Blending starch with synthetic polymers such as PVA enhances the physicochemical stability and electrospinnability of the final composite [18]. Furthermore, the incorporation of bioactive agents, such as CuO NPs synthesized using algal extracts, into starch/PVA matrices can lead to hybrid scaffolds with augmented biological functions [19].

In this context, the present study aims to fabricate starch/PVA-based electrospun nanofibrous scaffolds embedded with biosynthesized CuO NPs for potential biomedical applications [20]. A key novelty of this research lies in the use of ultrasound-assisted extraction to obtain bioactive compounds from *Ectocarpales* algae, thereby enhancing the efficiency of phytochemical-mediated nanoparticle synthesis [21]. The synthesized CuO NPs were characterized using a suite of analytical techniques including UV-Visible spectroscopy, Fourier-transform infrared spectroscopy (FTIR), X-ray Diffraction (XRD), Scanning Electron Microscopy (SEM), zeta potential analysis, and thermogravimetric analysis to elucidate their structural, morphological, and thermal properties [22, 23]. The nanofiber composites were also subjected to similar characterizations to assess their homogeneity, fiber morphology, crystallinity, and thermal behavior [24].

To further explore the biomedical potential of the developed materials, their anti-inflammatory efficacy was assessed using two in vitro assays—protein denaturation inhibition and xanthine oxidase inhibition [25]. These assays are widely recognized as reliable models for screening anti-inflammatory agents due to their correlation with inflammation pathways in vivo [26]. Inflammation is a central biological response to injury and infection, but uncontrolled inflammation can lead to tissue damage and delay healing [27]. Hence, materials that can mitigate inflammatory responses without inducing toxicity are of great interest in regenerative medicine and wound management [28].

By integrating the bioactivity of marine-derived phytochemicals with the structural advantages of nanofiber scaffolds, this study endeavors to contribute to the development of a new class of multifunctional biomaterials. Such hybrid systems may serve as intelligent platforms for localized and controlled therapeutic delivery, while also providing structural support for cellular attachment and tissue regeneration [29]. Moreover, the environmentally sustainable approach adopted in the synthesis and fabrication processes aligns with the growing emphasis on green chemistry and circular bioeconomy in biomedical material development [30].

2.MATERIALS AND METHODS

2.1. Chemicals and materials

Marine brown algae of the *Ectocarpales* order, harvested from Rameswaram, Tamil Nadu, were utilized as a sustainable biological resource for the green synthesis of CuO NPs. Copper (II) sulfate pentahydrate ($CuSO_4 \cdot 5H_2O$, Sigma-Aldrich) was used as the metal salt precursor. PVA with a molecular weight of approximately 145,000 and commercially sourced starch were employed for fabricating electrospun nanofibers using a HOLMARC HO-NFES-040 electrospinning system. All additional solvents and reagents, procured from Sigma-Aldrich and Merck, were of analytical grade and used as received without further purification. Characterization techniques included UV-visible spectroscopy, FT-IR spectroscopy, XRD using a Bruker D8 Advance system, SEM using JEOL JSM-IT800, zeta potential measurement with a Malvern Zetasizer Ultra, and thermal analysis using a PerkinElmer TGA 8000. Anti-inflammatory properties were evaluated using established standard methods.

2.2. Collection and preparation of *Ectocarpales* algae

Ectocarpales brown algae were hand-collected from intertidal areas along the Rameswaram coast. To remove contaminants, algae were thoroughly rinsed with tap water to eliminate debris and sand particles, followed by washing with distilled water to remove remaining impurities. The cleaned biomass, weighing approximately 100 g, was chopped into small pieces and subjected to shade drying at ambient temperature (~28°C) for a period of two weeks. The desiccated biomass was finely powdered using a mechanical grinder and stored in airtight containers protected from moisture for subsequent use.

2.3. Ultrasound-Assisted extraction of bioactive compounds

To isolate bioactive molecules, 2 g of algal powder was suspended in 50 mL of Milli-Q water in a sterile beaker. The suspension underwent ultrasonication in a LABQUEST ultrasonic bath (Borosil; Serial No. 941032329018) maintained at 60°C for 45 minutes. Ultrasonic energy facilitated the breakdown of cell walls and enhanced the release of intracellular phytochemicals. The mixture was then filtered through Whatman No. 1 filter paper under sterile conditions. The resulting filtrate was stored in a clean container at 10°C for immediate use or freeze-dried for long-term preservation, yielding a powdered extract [31, 32].

2.4. Green synthesis of CuO NPs

CuO NPs were synthesized via a bio-reduction process using algal extract. A 0.1 M aqueous solution of $CuSO_4 \cdot 5H_2O$ (50 mL) was mixed with 10 mL of algal extract (prepared by dissolving 10 mg of lyophilized extract in 10 mL Milli-Q water) in a 5:1 ratio. This mixture was magnetically stirred at 650 rpm and 60°C for two hours. A color change from deep blue to pale bluish-green signaled nanoparticle formation. The resulting colloidal solution was washed thrice with double-distilled water to remove excess phytochemicals and unreacted salts. The cleaned nanoparticles were lyophilized for 48 hours to obtain stable CuO nanopowder for further analysis and scaffold fabrication [9].

2.5. Fabrication of starch/PVA nanofibers embedded with CuO NPs

Hybrid nanofibrous mats were fabricated by dissolving 15% (w/w) PVA in distilled water under constant heating and stirring. Once fully solubilized, 100 mg each of starch and biosynthesized CuO NPs were added to the solution. The blend was stirred at 50°C for 2.5 hours to ensure uniform dispersion. The electrospinning process was carried out using the HOLMARC HO-NFES-040 apparatus. The polymeric solution was transferred into a syringe fitted with a 0.84 mm needle. Optimal electrospinning parameters included a voltage of 11.5 kV, a distance of 12.3 cm between the nozzle and collector, and a feed rate of 0.4 mL/h. Fibers were collected on aluminum foil for 6 to 8 hours at room temperature, forming uniform nanofibrous mats [33-35].

2.6. Physicochemical characterization methods

2.6.1. UV-Visible spectral analysis

Optical characteristics of the algal extract, CuO NPs, and nanofiber composites were examined using a VIS SPEC V-730 spectrophotometer. Absorbance was recorded from 200 to 800 nm, with deionized water as the blank [36].

2.6.2. FT-IR spectroscopic analysis

FT-IR spectra were recorded using a PerkinElmer Spectrum Two instrument in ATR mode. Spectral data were obtained in the 4000 to 400 cm^{-1} range, with a resolution of 4 cm^{-1}. Each spectrum was averaged over 64 scans to improve signal quality and identify functional group interactions involved in nanoparticle synthesis and scaffold formation [37].

2.6.3. XRD analysis

XRD analysis was performed using a Bruker D8 Advance diffractometer with CuKα radiation (λ = 1.5406 Å), operating at 40 kV and 40 mA. Data were collected over a 2θ range of 5° to 90° with a step size of 0.029649° to identify crystalline phases in both nanoparticles and composite materials [37].

2.6.4. SEM analysis

The morphology and surface features of the CuO NPs and electrospun nanofibers were visualized using a JEOL JSM-IT800 SEM . Samples were gold-coated to enhance conductivity and image clarity. SEM images were evaluated to assess fiber structure, nanoparticle distribution, and overall surface morphology [38].

2.6.5. TGA

Thermal behavior was assessed with a PerkinElmer TGA 8000 analyzer. Samples (~5 mg) were heated from ambient temperature to 550°C at a rate of 15°C/min under a nitrogen atmosphere. Thermal degradation profiles were used to determine material stability and composition [39].

2.6.6. Particle size and zeta potential analysis

Dynamic and electrophoretic light scattering techniques were employed using a Malvern Zetasizer Ultra to determine the particle size distribution and zeta potential of the CuO NPs. These measurements provided insight into the stability and dispersion properties of the colloidal particles [40].
All characterization data are available on Mendeley Data (DOI: 10.17632/m7jzmb7mr9.1).

2.7. Anti-inflammatory activity assays

2.7.1. Protein denaturation inhibition assay

To evaluate the inhibition of heat-induced protein denaturation, a modified standard method was followed. A reaction mixture comprising 0.45 mL of 5% bovine serum albumin solution and 0.05 mL of test samples (algal extract, CuO NPs, starch/PVA/CuO nanoscaffolds, and diclofenac sodium as reference) was prepared. Sample concentrations were 25, 50, 75, and 100 µg/mL. The mixture pH was adjusted to 6.3 with 1 N HCl, incubated at 37°C for 20 minutes, and then heated at 57°C for 3 minutes. After cooling to room temperature, absorbance at 660 nm was measured to assess protein denaturation [41].

2.7.2. Xanthine oxidase inhibition assay

This assay was adapted from a standard method to assess xanthine oxidase inhibition. Test solutions (0.3 mL) containing algal extract, CuO NPs, composite nanoscaffolds, or diclofenac sodium were mixed with 0.5 mL of 0.15 mM xanthine solution (in phosphate buffer, pH 7.5) and 0.2 mL of xanthine oxidase enzyme (0.1 U/mL). After 15 minutes of incubation at 25°C, absorbance was measured at 295 nm. A parallel blank without enzyme served as a control [42].

2.8. Statistical analysis

Experimental data were statistically analyzed using SPSS version 25.0 and GraphPad Prism version 9.0. Triplicate measurements were reported as mean ± standard deviation. One-way ANOVA was applied for group comparisons, with Tukey's or Dunnett's post hoc tests based on the analysis requirement. A p-value < 0.05 indicated statistical significance. The Shapiro–Wilk test assessed data normality; if violated, data were log-transformed prior to analysis. Pearson's correlation coefficient was employed to evaluate relationships among variables. All statistical outcomes were interpreted at a 95% confidence level to ensure validity and accuracy [43].

3.RESULTS

3.1. UV–visible spectroscopic characterization

The UV–Visible absorption profiles (Figure 1) for the *Ectocarpales* extract and the synthesized CuO NPs were acquired using a JASCO UV-VIS spectrophotometer (Model V-730), covering the wavelength span from 200 to 800 nm. Deionized water functioned as the blank reference. The *Ectocarpales* extract exhibited a broad absorption region between 200 and 400 nm, peaking near 300 nm with an absorbance of 0.93687. This absorption peak is indicative of π-π* electronic transitions, typically associated with phenolic compounds, flavonoids, and chlorophyll derivatives present in marine algae. A consistent decline in absorbance was noted from 400 to 800 nm, suggesting minimal interaction in the visible spectrum, consistent with a lower presence of extended conjugated systems [44, 45].

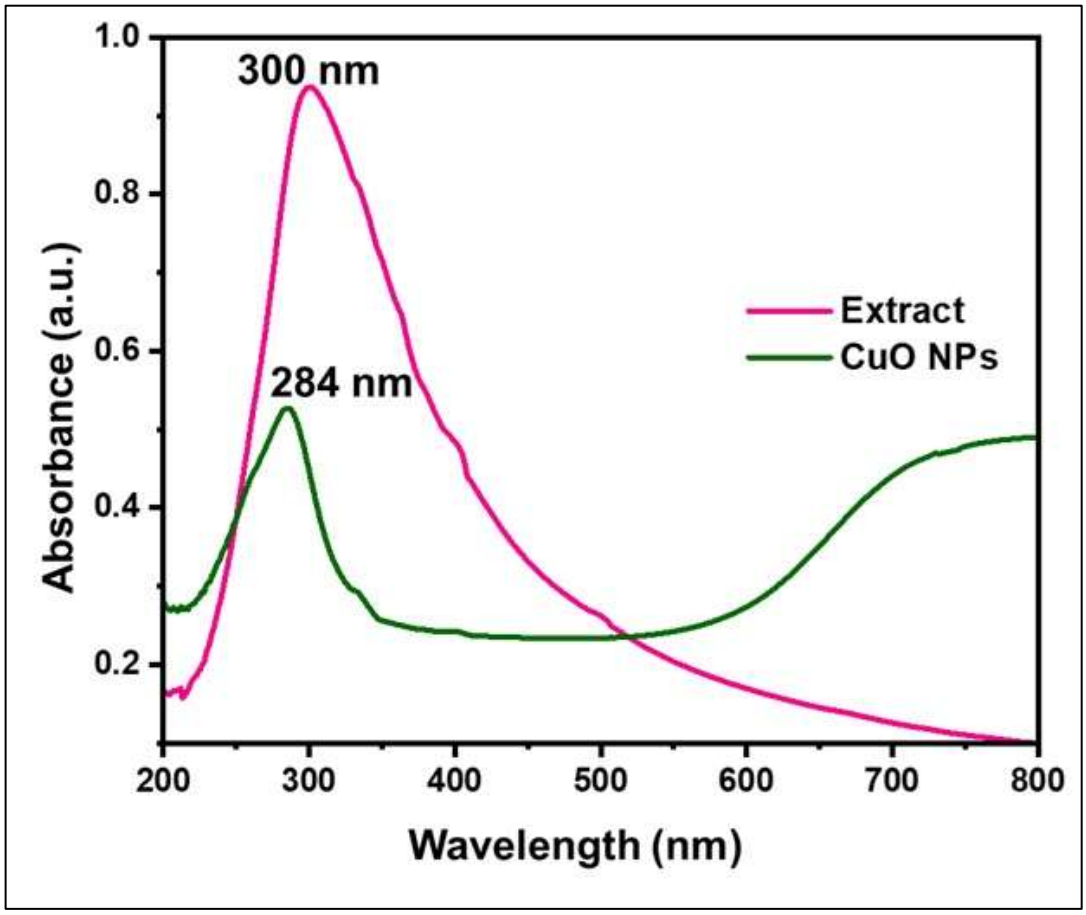

Figure 1. UV–Visible Spectroscopy analysis of algae extracts and CuO NPs

Conversely, the CuO NPs displayed a sharp UV absorption edge, with a dominant peak at 200 nm (absorbance: 0.53295), reflecting the intrinsic bandgap and possible surface plasmon resonance effects. The absorbance gradually diminished across the higher wavelength region, a characteristic trait of semiconducting nanoparticles. The clear spectral divergence between the algal extract and the synthesized CuO NPs underscores their differing material natures—organic for the extract and inorganic for the NPs. These absorption spectra substantiate the successful synthesis and distinct optical identities of the extract and CuO NPs [46].

3.2. FT-IR spectral analysis

FT-IR spectroscopy (Figure 2) of both CuO NPs and the fabricated nanoscaffolds was performed using a PerkinElmer Spectrum Two spectrometer in Attenuated Total Reflectance (ATR) mode, ranging from 4000 to 400 cm^{-1} with a 4 cm^{-1} resolution over 64 scans. For CuO NPs, notable vibrational peaks were recorded at 3216 cm^{-1}, associated with O–H stretching from moisture adsorption, and at 1511 cm^{-1}, likely arising from C=O stretching or aromatic ring vibrations. A prominent band at 860 cm^{-1} corresponded to Cu–O stretching, confirming the formation of copper oxide bonds and possible residual organics from the synthesis [47-49].

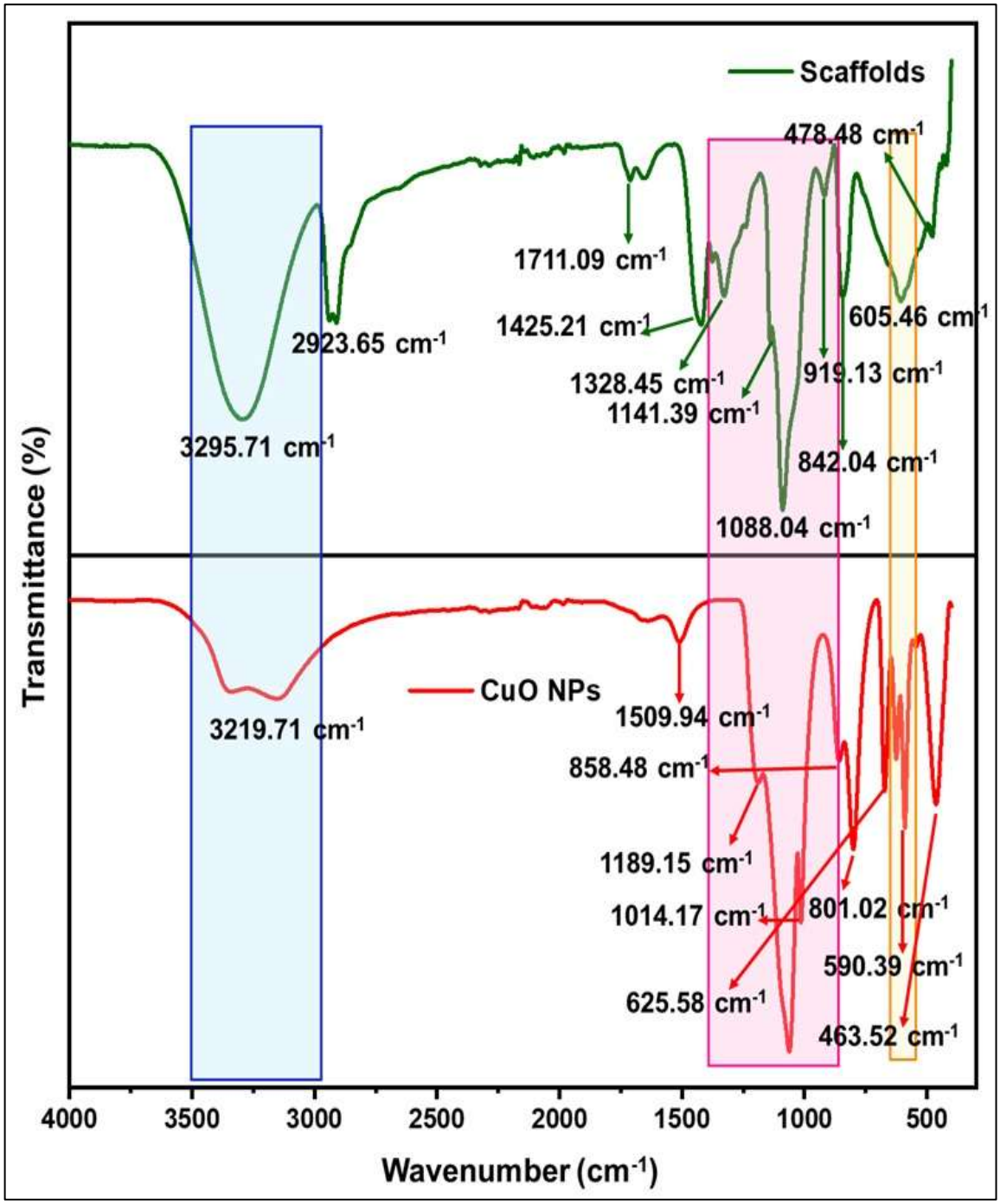

Figure 2. FTIR analysis of CuO NPs and starch/PVA/CuONPs nanoscaffolds

The nanoscaffold spectrum showed broader, more complex bands, with a major peak at 3298 cm^{-1} indicating O–H and/or N–H stretching typical of polymeric substances. A distinct band at 2107 cm^{-1} suggested the presence of C≡N or cumulative C=C=N functionalities. Peaks at 1652 cm^{-1} and 1327 cm^{-1} were linked to C=O stretching and O–H or C–N bending modes, respectively. Additional absorption bands at 840 cm^{-1} and 607 cm^{-1} implied glycosidic bonding and inorganic-polymeric interactions. These spectra verified the successful formation of CuO NPs and their integration into a polymer matrix, as evidenced by distinctive vibrational features [50].

3.3. XRD analysis

XRD (Figure 3) for CuO NPs and nanoscaffolds was conducted with a Bruker D8 Advance diffractometer using CuKα radiation (λ = 1.5406 Å) at 40 kV and 40 mA. The diffraction angles (2θ) ranged from 5° to 90° with a step size of 0.029649°. The CuO NPs presented 25 distinct diffraction peaks, with significant reflections at 26.201° (d = 3.398 Å), 20.312° (d = 4.369 Å), and 36.148° (d = 2.483 Å), consistent with the monoclinic tenorite phase of CuO, as referenced by JCPDS card No. 05-0661. Sharp peaks and narrow full-width at half maximum (FWHM) values indicated a high degree of crystallinity [51, 52].

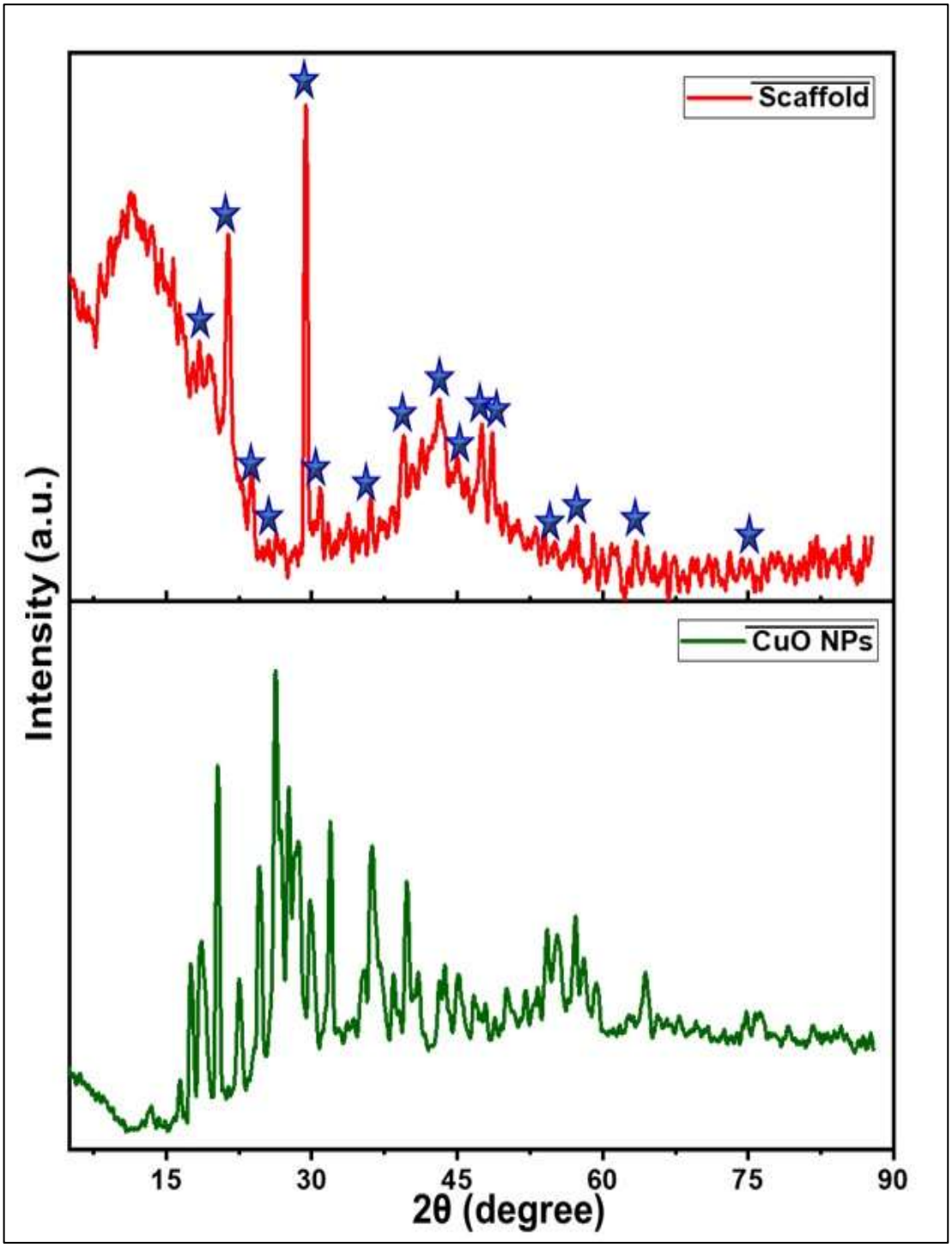

Figure 3. XRD analysis of CuO NPs and starch/PVA/CuONPs nanoscaffolds

Nanoscaffolds exhibited 14 diffraction peaks, with dominant signals at 21.199° (d = 4.188 Å) and 30.844° (d = 2.897 Å), representing a semi-crystalline polymeric structure, calculated to consist of 15.9% crystalline and 84.1% amorphous regions. Broader diffraction peaks with increased FWHM values suggested a lower structural order, potentially due to CuO NP dispersion within the polymer network. The absence of overlapping peaks confirmed both the structural purity and the integrity of the CuO NPs and nanoscaffolds [53].

3.4. SEM analysis

SEM (Figure 4) performed with a JEOL JSM-IT800 NANO SEM provided morphological insights into the synthesized CuO NPs and nanofibrous scaffolds. CuO NPs exhibited predominantly spherical to slightly irregular shapes, with particle sizes ranging from 50 to 200 nm. Minor agglomeration was observed, likely due to high surface energy, though discrete particles remained visible [54].

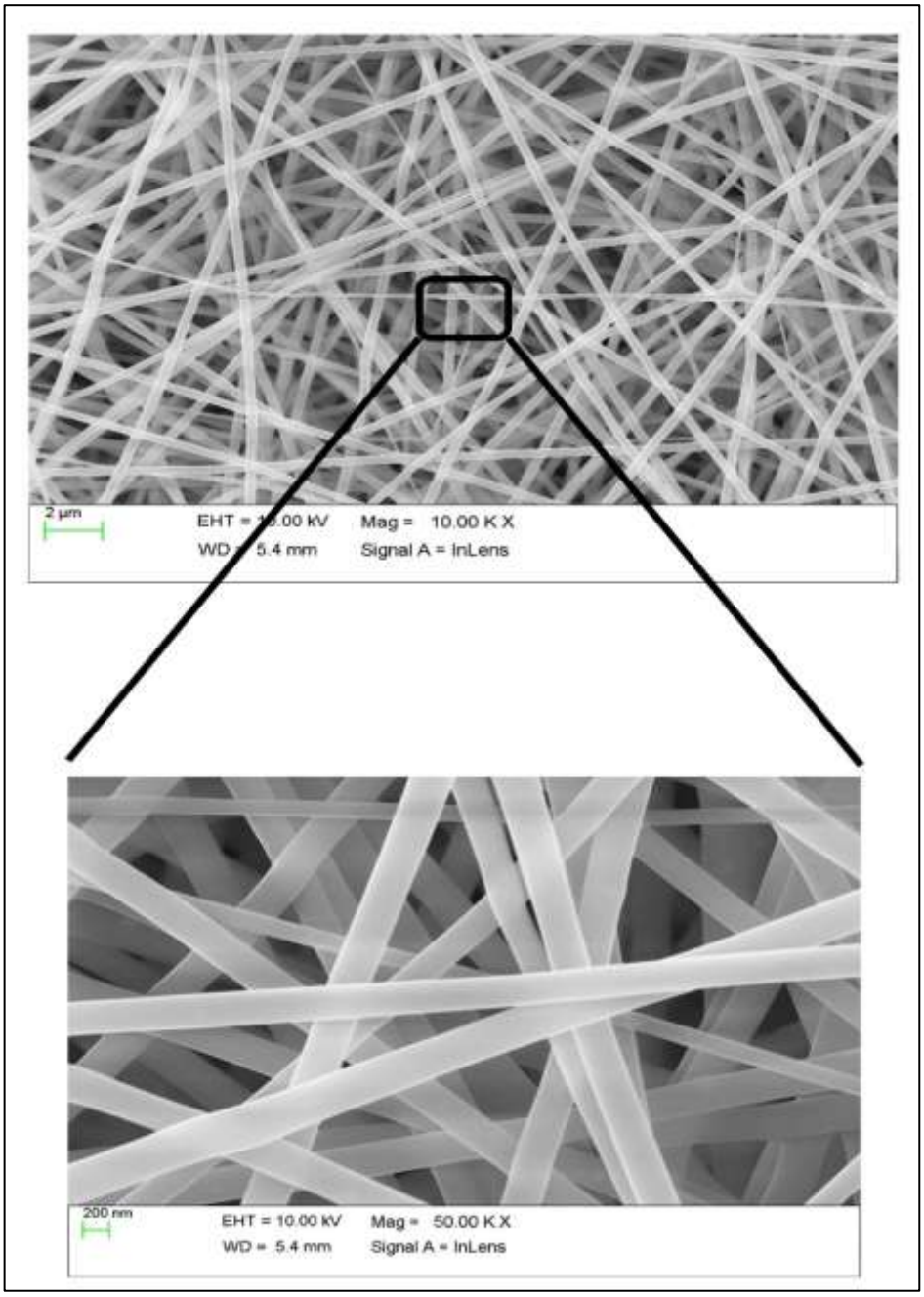

Figure 4. SEM analysis of starch/PVA/CuONPs nanoscaffolds

The nanoscaffolds revealed a fibrous network structure characterized by porosity and interconnectivity. The fibers measured between 70 and 90 nm in diameter, exhibiting smooth surfaces and occasional bead formation, indicative of well-optimized electrospinning conditions. Embedded bright particles were discerned along the fiber surfaces, confirming even distribution of CuO NPs throughout the scaffold matrix. This integrated nanostructure, featuring hierarchical porosity and effective nanoparticle embedding, demonstrates promising potential for biomedical applications, particularly in tissue regeneration and wound dressing. Minimal aggregation affirmed proper nanoparticle incorporation [55].

3.5. TGA analysis

Thermal gravimetric analysis (Figure 5) was conducted on the nanoscaffolds using a PerkinElmer TGA 8000 instrument. A 1.012 mg sample was subjected to a heating protocol from room temperature up to 600°C in a nitrogen atmosphere, at a rate of 15°C/min. The thermogram displayed a multi-step decomposition profile. An initial mass loss of 3.581% occurred below 100°C, attributed to moisture and solvent evaporation. The major degradation stage was noted at 336.92°C, corresponding to decomposition of the polymer components (e.g., starch or PVA). Complete degradation was achieved by 400.84°C, resulting in a residual mass of 31.102%, which was ascribed to the CuO NPs content [56].

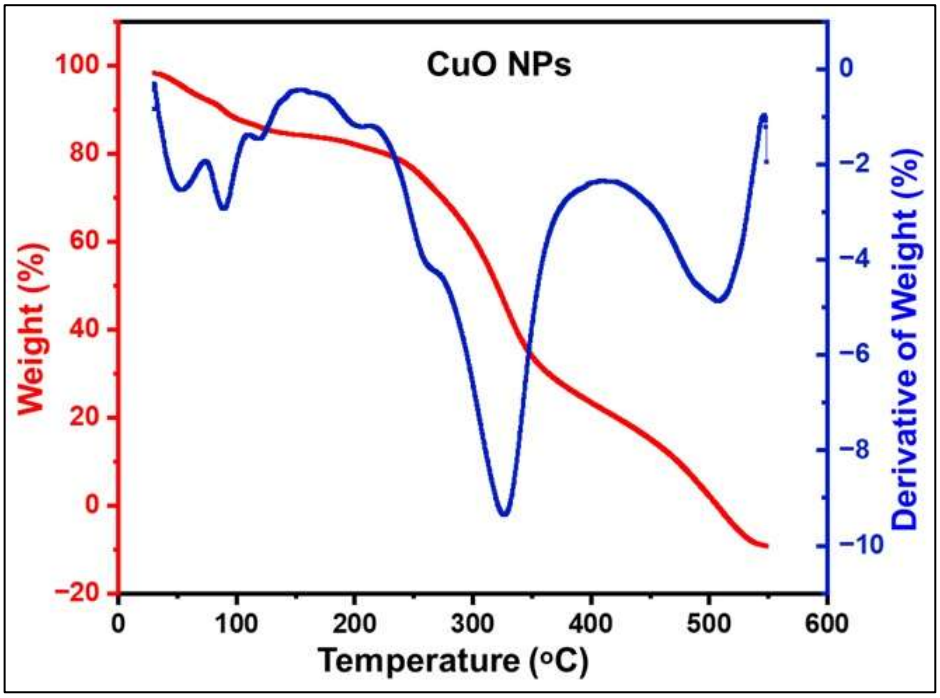

Figure 5. TGA analysis of starch/PVA/CuONPs nanoscaffolds

The elevated thermal degradation temperature and residual content highlight the scaffold's thermal stability, making it suitable for applications in thermally demanding environments. These results further emphasize the structural robustness and composite composition of the developed nanoscaffold [57].

3.6. Dynamic light scattering (DLS) and zeta potential

DLS and zeta potential measurements were used to evaluate the size distribution and surface charge of CuO NPs via a Malvern Zetasizer Ultra system. The DLS analysis showed a mean hydrodynamic diameter (Z-average) of 79.8 nm (Figure 6) and a polydispersity index (PDI) of 0.475, indicating moderate size variation. Zeta potential (Figure 7) readings revealed an average surface charge of +14.03 mV, with two main populations observed at +10.94 mV and +28.06 mV. The positive charge suggests a cationic surface nature, likely due to residual organic capping agents from the biosynthesis.

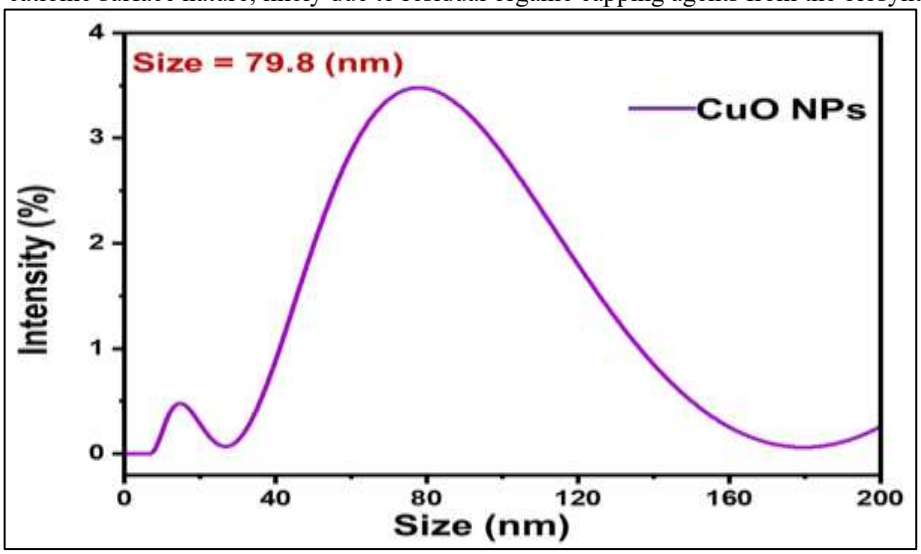

Figure 6. Particle size analysis of CuO NPs

The suspension demonstrated a conductivity of 0.1179 mS/cm and a quality factor of 2.084, pointing to a relatively stable colloidal state. Despite some presence of larger aggregates, the CuO NPs exhibited acceptable dispersibility and surface stability, supporting their applicability in biomedical and environmental fields. These metrics offer essential information about the physical characteristics and potential interactions of the nanoparticles in colloidal systems [58].

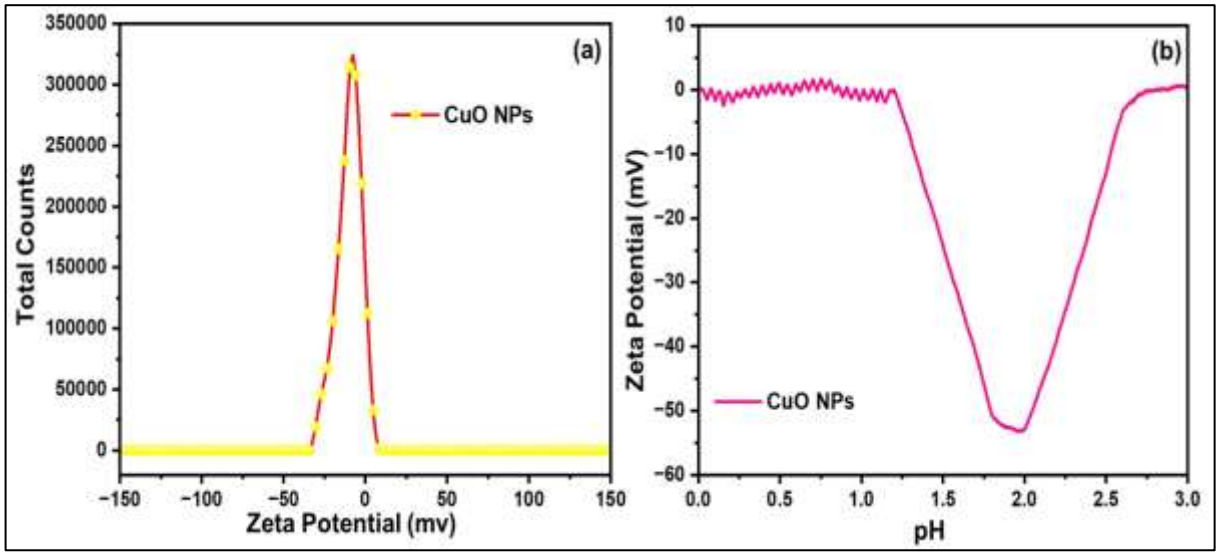

Figure 7. Zeta potential analysis of CuO NPs

3.7. Anti-inflammatory capability

3.7.1. Protein denaturation inhibition assay

The anti-inflammatory potential of algal extract, CuO NPs, and starch/PVA/CuO-NPs nanoscaffolds was evaluated using the protein denaturation inhibition assay (Figure 8). The results demonstrated concentration-dependent inhibition of bovine serum albumin (BSA) denaturation. At 25 µg/mL, the algal extract exhibited 18.37% inhibition, while CuO NPs and nanoscaffolds showed 22.37% and 25.37% inhibition, respectively. As the concentration increased to 50 µg/mL, the inhibition percentages rose to 33.77% (extract), 37.77% (CuO NPs), and 39.77% (nanoscaffolds). At 75 µg/mL, the inhibition further increased to 52.89% (extract), 57.89% (CuO NPs), and 61.89% (nanoscaffolds). The highest concentration (100 µg/mL) resulted in inhibition values of 62.57% (extract), 68.57% (CuO NPs), and 78.57% (nanoscaffolds). These findings indicate that the nanoscaffolds exhibited the strongest anti-inflammatory effect, followed by CuO NPs and the algal extract [59].

A second set of measurements at the same concentrations showed slight variations, reinforcing the trend. At 25 µg/mL, the inhibition was 18.16% (extract), 24.16% (CuO NPs), and 26.16% (nanoscaffolds). At 50 µg/mL, the values were 34.57%, 39.57%, and 41.57%, respectively. The 75 µg/mL concentration yielded 48.69%, 54.69%, and 61.69% inhibition, while 100 µg/mL resulted in 63.37%, 70.37%, and 77.37% inhibition. The consistent enhancement in inhibition with increasing concentration highlights the dose-dependent efficacy of all three samples, with nanoscaffolds outperforming the others [60].

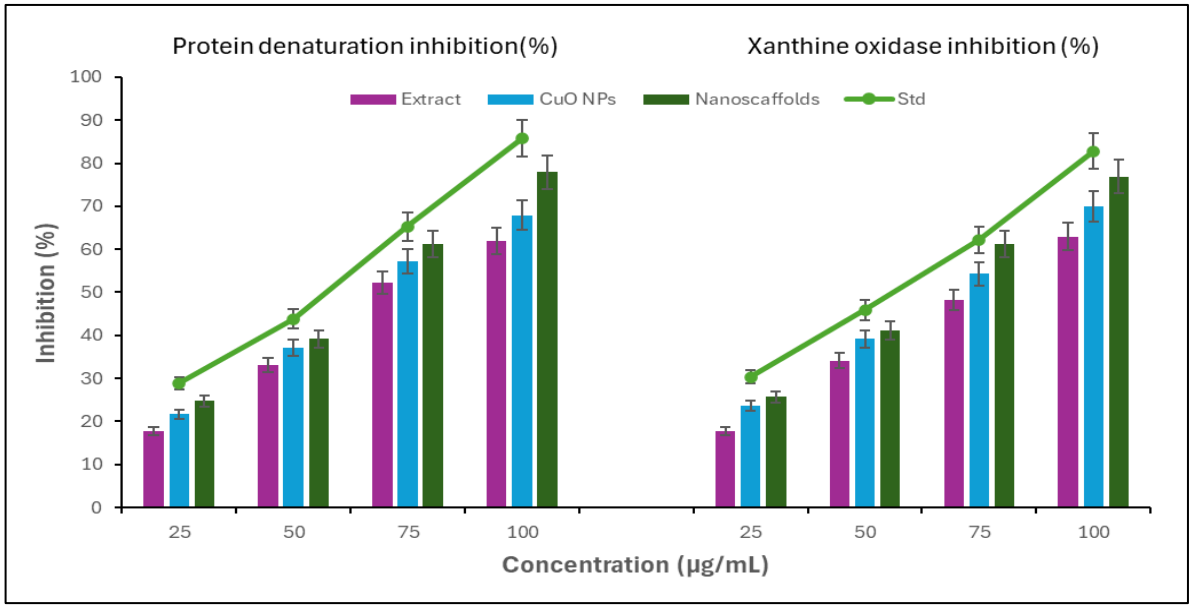

Figure 8. Anti-inflammatory potential of algal extract, CuO NPs and starch/PVA/CuO-NPs nanoscaffolds

3.7.2. Xanthine oxidase inhibition assay

The xanthine oxidase inhibition assay (Figure 8) was used to assess the anti-inflammatory activity by measuring the suppression of uric acid formation. The results followed a similar concentration-dependent trend. At 25 µg/mL, the algal extract inhibited xanthine oxidase by 18.37%, while CuO NPs and nanoscaffolds showed 22.37% and 25.37% inhibition,

respectively. Increasing the concentration to 50 µg/mL enhanced the inhibition to 33.77% (extract), 37.77% (CuO NPs), and 39.77% (nanoscaffolds). At 75 µg/mL, the values further increased to 52.89%, 57.89%, and 61.89%, while the highest concentration (100 µg/mL) resulted in 62.57%, 68.57%, and 78.57% inhibition.

The second set of measurements confirmed these trends, with inhibition percentages of 18.16%, 24.16%, and 26.16% at 25 µg/mL, rising to 34.57%, 39.57%, and 41.57% at 50 µg/mL. The 75 µg/mL concentration showed 48.69%, 54.69%, and 61.69% inhibition, while 100 µg/mL exhibited 63.37%, 70.37%, and 77.37% inhibition. These results suggest that the nanoscaffolds possess superior xanthine oxidase inhibitory activity compared to CuO NPs and the algal extract, reinforcing their potential as effective anti-inflammatory agents.

Both assays demonstrated that the starch/PVA/CuO-NPs nanoscaffolds exhibited the highest anti-inflammatory activity, followed by CuO NPs and the algal extract. The inhibition was concentration-dependent, with higher efficacy observed at increased concentrations. These findings suggest that the nanoscaffolds could serve as a promising anti-inflammatory therapeutic agent, potentially surpassing the effectiveness of conventional treatments. Further studies could explore their mechanisms of action and in vivo efficacy.

4.DISCUSSION

The characterization and functional evaluation of CuO NPs synthesized from *Ectocarpales* extract, and their subsequent integration into starch/PVA-based nanoscaffolds, provided a comprehensive understanding of their physicochemical, morphological, and biological properties. The results indicate successful synthesis and functionalization, as well as promising anti-inflammatory potential [61-63].

The UV–Visible spectroscopic analysis effectively differentiated the optical behaviors of the algal extract and the synthesized CuO NPs [64]. The algal extract exhibited a broad absorption band between 200 and 400 nm, with a distinct peak at 300 nm, typically attributed to π-π* transitions found in polyphenols, flavonoids, and chlorophyll derivatives [65]. This spectral profile supports the presence of diverse phytochemicals that may act as both reducing and stabilizing agents during nanoparticle formation. In contrast, the CuO NPs demonstrated a sharp absorption peak at 200 nm, indicative of their intrinsic bandgap and possibly surface plasmon resonance phenomena. The decreased absorbance in the visible range for both samples confirmed minimal optical interference from conjugated systems, affirming the organic nature of the extract and the inorganic signature of CuO NPs. These contrasting profiles confirm the transformation from phytochemical-rich extract to metallic oxide nanoparticles, with distinct optoelectronic properties suitable for biomedical applications [66].

FT-IR spectral analysis revealed detailed insights into the functional groups associated with CuO NPs and nanoscaffolds. The CuO NPs exhibited characteristic peaks corresponding to O–H stretching, C=O vibrations, and most crucially, Cu–O bonds at 860 cm^{-1}, affirming the successful formation of copper oxide. In the nanoscaffold, broader and more intense bands were observed, such as O–H and N–H stretching around 3298 cm^{-1}, and signals for carbonyl and bending vibrations between 1652 cm^{-1} and 1327 cm^{-1}. The presence of peaks at 840 cm^{-1} and 607 cm^{-1} suggested interactions between inorganic particles and the polymeric matrix. The formation of new vibrational bands in the nanoscaffold spectrum indicates the incorporation of CuO NPs into the polymer structure and possibly the formation of hydrogen bonds and electrostatic interactions between the polymers and metal oxide [67, 68].

The XRD analysis offered critical data on the crystalline properties of both CuO NPs and nanoscaffolds [69]. The CuO NPs displayed sharp, well-defined peaks consistent with the monoclinic phase of tenorite CuO, verified using standard JCPDS references. Narrow full-width at half-maximum (FWHM) values indicated high crystallinity. Upon incorporation into nanoscaffolds, the number of diffraction peaks decreased, and their broadening suggested a reduction in crystalline order. The calculated composition of the scaffold showed 15.9% crystalline and 84.1% amorphous content, a typical trait of polymer matrices. Importantly, the absence of overlapping peaks between the polymer and the CuO NPs verified the structural integrity of each component and confirmed their successful combination without compromising crystalline identity [70].

SEM offered visual confirmation of morphology. The CuO NPs were predominantly spherical with minor irregularities and exhibited size distributions between 50 to 200 nm. Some agglomeration was observed, which is common for metallic nanoparticles due to high surface energy. The nanoscaffolds, on the other hand, presented a highly porous, interconnected fibrous structure, with diameters between 70 to 90 nm. The smooth fibers and minimal bead formation reflected optimal electrospinning conditions. Bright particles observed along the fibers confirmed homogeneous embedding of CuO NPs within the scaffold. This architecture is beneficial for biomedical uses, as porosity and uniform nanoparticle distribution are critical for cell adhesion, nutrient transport, and sustained drug release [71, 72].

Thermal Gravimetric Analysis (TGA) highlighted the thermal stability of the nanoscaffold. A minor weight loss occurred below 100°C due to moisture evaporation. A significant degradation stage was noted near 337°C, associated with decomposition of organic polymer constituents, while the process completed by 400°C. The presence of 31.1% residual mass post-degradation attributed to CuO NPs emphasized their stability under heat and confirmed their successful integration. These data indicate that the nanoscaffolds are thermally robust and suitable for high-temperature biomedical applications such as sterilization processes [73].

DLS and zeta potential measurements provided additional physicochemical data [74]. The average hydrodynamic diameter was found to be 79.8 nm, while a moderate polydispersity index (0.475) suggested acceptable size uniformity. The zeta potential of +14.03 mV indicated moderately stable colloidal suspension, with cationic surface properties likely resulting from phytochemical capping agents. These properties enhance cellular interactions, making the particles promising candidates for biological applications [75].

The anti-inflammatory studies further strengthened the therapeutic potential of the synthesized materials [76]. In the protein denaturation inhibition assay, all three materials algal extract, CuO NPs, and nanoscaffolds exhibited dose-dependent inhibition. Notably, the nanoscaffolds demonstrated the highest inhibition percentages at each concentration, reaching up to 78.57% at 100 µg/mL. This suggests a synergistic effect between the scaffold components and CuO NPs. Similarly, in the xanthine oxidase inhibition assay, the nanoscaffolds again outperformed both the extract and the standalone NPs, confirming their superior anti-inflammatory capacity [42]. These findings highlight the enhanced bioactivity resulting from nanoparticle incorporation into a biocompatible matrix.

The combination of characterization techniques confirms the successful synthesis of CuO NPs, their stable integration into starch/PVA nanoscaffolds, and their promising anti-inflammatory activity. The developed nanoscaffolds possess desirable physicochemical and biological traits optical distinctiveness, thermal resilience, structural porosity, and potent bioactivity—making them suitable candidates for applications in wound healing, inflammation control, and tissue engineering.

5.CONCLUSION

The present study successfully demonstrates the eco-friendly synthesis of CuO NPs using *Ectocarpales* extract and their effective incorporation into starch/PVA nanoscaffolds. Comprehensive characterization confirmed the formation, stability, and uniform distribution of CuO NPs within the biopolymer matrix. Spectroscopic, thermal, and microscopic analyses established the structural integrity, thermal resistance, and morphological features suitable for biomedical applications. Notably, the anti-inflammatory assays revealed that the starch/PVA/CuO nanoscaffolds exhibited superior inhibitory activity against protein denaturation and xanthine oxidase, outperforming the individual components. These results suggest a synergistic effect between the bioactive compounds in the algal extract and the nanocomposite scaffold. The enhanced anti-inflammatory potential, along with the biocompatibility and degradability of the scaffold materials, underscores their applicability in advanced wound healing and tissue repair. Overall, this green nanotechnology approach offers a sustainable, cost-effective, and therapeutically promising strategy for developing novel biomaterials in regenerative medicine.

Ethical Declaration: Not applicable for this study.

Funding: Not available for this study.

Conflicts of Interest: The authors declare no conflicts of interest.

Data Availability Statement: The full dataset of physiochemical characterization associated with this work is published in Mendeley Data [Dataset] Structural and functional profiling of starch-polymer nanoscaffolds enhanced with *Ectocarpales*-derived biogenic copper oxide nanoparticles (DOI: 10.17632/m7jzmb7mr9.1). **Disclosure**: The material characterization data and figures (e.g., UV, SEM, FTIR, XRD, TGA, Zeta Potential and particle sizer) presented here were generated from a common dataset and are being reused across multiple related studies on nanomaterials. All biological analyses and conclusions are original to each manuscript.

REFERENCES

1. Panneerselvam S, Viswaja K, Deepa E, Prathiba S, Rebecca FS, Nivedha RP, Rajagopal P, Veeraraghavan VP, Sridevi G, Palanisamy CP, Jayaraman S. Hypoglycemic Potential of Acalypha indica in Streptozotocin-Induced Type 2 Diabetic Rats. International Journal of Drug Delivery Technology. 2026; 16(26s):1038-1047.
2. Panneerselvam S, Viswaja K, Prathiba S, Rebecca FS, Nivedha RP, Rajagopal P, Fathima SJH, Veeraraghavan VP, Sridevi G, Palanisamy CP, Jayaraman S. Acalypha Indica Attenuates Insulin Resistance in STZ-Induced Type 2 Diabetic Male Rats: Mechanistic Study. International Journal of Drug Delivery Technology. 2026; 16(26s):1027-1037.
3. Manju NE, Natarajan A, Rebecca FS, Nivedha RP, Hemalatha R, Rajagopal P, Murali R, Veeraraghavan VP, Sridevi G, Palanisamy CP, Jayaraman S. Effect of Seendhil polyherbal formulation in attenuating type-2 diabetes in STZ-induced experimental rats. International Journal of Drug Delivery Technology. 2026; 16(26s):981-989.
4. Manju NE, Natarajan A, Rebecca FS, Nivedha RP, Hemalatha R, Rajagopal P, Murali R, Veeraraghavan VP, Sridevi G, Palanisamy CP, Jayaraman S. Molecular mechanism to identify the effects of Seendhil polyherbal preparation on IRS-1/AKT/GLUT4/NRF2-KEAP-1 mediated signaling in SFZ-induced type-2 diabetic adult male rats. International Journal of Drug Delivery Technology. 2026;16(26s):972-980.
5. Palanisamy CP, Poompradub S, Sansanaphongpricha K, Jayaraman S, Subramani K, Sonsudin F. Biosynthesis of silver nanoparticles (AgNPs) using ethanolic extract of Nigella sativa (L.) seeds promotes wound healing via PDGF and VEGF signalling pathways activation. Biocatalysis and Agricultural Biotechnology. 2023; 54: 102970.
6. Palanisamy CP, Pei JJ, Phaniendra A, Venkata AAN, Jayaraman S, Veeraragahavan VP, Sridevi G, Roy JR, Janaki CS, Thalamati D, Mironescu M, Luo Q, Chai Y, Long Q. New Strategy of Neurodegenerative Disease Treatment with Extracellular Vesicles (EVs) Derived from Mesenchymal Stem Cells (MSCs). Theranostics. 2023; 13(12):4138-4165.
7. Yadalam PK, Arumuganainar D, Natarajan PM, Ardila CM. Artificial intelligence-powered prediction of AIM-2 inflammasome sequences using transformers and graph attention networks in periodontal inflammation. Scientific Reports. 2025; 15: 8733.

8. Yadalam PK, Chatterjee S, Natarajan PM, Ardila CM. Comparison of light gradient boosting and logistic regression for interactomic hub genes in Porphyromonas gingivalis and Fusobacterium nucleatum-induced periodontitis with Alzheimer's disease. Frontiers in Oral Health. 2025; 6:1463458.
9. Natarajan PM, Bhuminathan S, Leela B, Bindu K, Loganathan K, Ramachandran V. Smoking and its Role in Oral Cancer. Journal of Pharmacy and Bioallied Sciences 16(5): S4242-S4244.
10. Yadalam PK, Natarajan PM, Ardila CM. Variational graph autoencoder for reconstructed transcriptomic data associated with NLRP3 mediated pyroptosis in periodontitis. Scientific Reports. 2025; 15: 1962.
11. Natarajan PM, Swamikannu B, Sivaraman NM, Stylin AGSQ. Prevention of Oral Cancer: A Comprehensive Guide. Journal of Pharmacy and Bioallied Sciences. 2024; 16(5): S4239-S4241.
12. Guo H, Liu Y, Wan T, Song D, Palanisamy CP, Geng J, Pei J, Özmen S, El-Aty AMA. Toward personalized cancer management: Role of precision nutrition–diet interventions. Journal of Functional Foods. 2024; 123: 106584.
13. Natarajan SR, Krishnamoorthy R, Alshuniaber MA, Al-Anazi KM, Farah MA, Rajagopal P, Palanisamy CP, Veeraraghavan VP, Jayaraman S. Identification of FOXM1 as a novel protein biomarker and therapeutic target for colorectal cancer progression: Evidence from immune infiltration and bioinformatic analyses. International Journal of Biological Macromolecules. 282 (Part 4): 137201.
14. Rajendran MS, Jayaraman S, Khan JM, Jasmine S, Prabhakaran RK, Raju MV, Chandrasekaran MK, Ahalliya RM, Kannappan P, Palanisamy CP, Kanniappan GV. Investigating the colon toxicity and carcinogenic role of monosodium glutamate compared with Dimethylhydrazine in male Wistar rats: Exploring the link to childhood colon cancer risk. Journal of King Saud University - Science. 2024; 36(11): 103507.
15. Kumarasamy RV, Natarajan PM, Umapathy VR, Roy JR, Rab SO, Saeed M, Panagal M, Mironescu M, Srinivasan GP, Palanisamy CP. Clinical Applications and Therapeutic Potentials of Advanced Nanoparticles: A Comprehensive Review on Completed Human Clinical Trials. Frontiers in Nanotechnology. 2024; 6:1479993.
16. Jin W, Pei JJ, Roy JR, Jayaraman S, Ahalliya RM, Kanniappan GV, Mironescu M, Palanisamy CP. Comprehensive review on single-cell RNA sequencing: A new frontier in Alzheimer's disease research. Ageing Research Reviews. 2024; 274: 102454.
17. Pei J, Palanisamy CP, Jayaraman S, Natarajan PM, Umapathy VR, Roy JR, Panagal M, Jayaraman S. Curcumin-loaded polymeric nanomaterials as a novel therapeutic strategy for Alzheimer's disease: A comprehensive review. Ageing Research Reviews. 2024; 99: 102393.
18. Pei J, Palanisamy CP, Jayaraman S, Natarajan PM, Umapathy VR, Roy JR, Thalamati D, Ahalliya RM, Kanniappan GV*, Mironescu M. A comprehensive review on starch-based Sustainable Edible Films Loaded with Bioactive Components for Food Packaging. International Journal of Biological macromolecules. 2024; 274 (Part-1): 133332.
19. Palanisamy CP, poompradub S, Sansanaphongpricha K, Subramani K, Sonsudin F. Increased expression levels of PDGF and VEGF magnify the wound healing potential facilitated by biogenic synthesis of silver nanoparticles. Nano-Structures & Nano-Objects. 2024; 39: 101236.
20. Pei J, Palanisamy CP, Jayaraman S, Natarajan PM, Umapathy VR, Roy JR, Thalamati D, Ahalliya RM, Kanniappan GV, Mironescu M. Proteomics Profiling of Extracellular Vesicle for Identification of Potential Biomarkers in Alzheimer's Disease: A Comprehensive Review. Ageing Research Reviews. 2024; 99: 102359.
21. Xi J, Wang T, Xian P, Liu X, Du M, Yang H, Palanisamy CP, Lin W, Long Q. Proteomic insights uncover enhanced neurotherapeutic potential in conditioned mesenchymal stem cell-derived extracellular vesicles. Extracellular Vesicle. 2024; 3: 100037.
22. Pei J, Natarajan PM, Umapathy VR, Swamikannu B, Sivaraman NM, Krishnasamy L, Palanisamy CP. Advancements in the synthesis and functionalization of zinc oxide-based nanomaterials for enhanced oral cancer therapy. Molecules. 2024; 29(11): 2706.
23. Gatasheh MK, Natarajan SR, Krishnamoorthy R, Alsulami TS, Rajagopal P, Palanisamy CP, Veeraraghavan VP, Jayaraman S. Molecular analysis to identify novel potential biomarkers as drug targets in colorectal cancer therapy: an integrated bioinformatics analysis. Molecular and Cellular Oncology. 2024; 11(1): 2326699.
24. Pei J, Yan Y, Jayaraman S, Rajagopal P, Natarajan PM, Umapathy VR, Gopathy S, Roy JR, Sadagopan CS, Thalamati D, Palanisamy CP, Mironescu M. A review on advancements in the application of starch-based nanomaterials in biomedicine: Precision drug delivery and cancer therapy. International Journal of Biological Macromolecules. 2024; 130746.
25. Pei JJ, Yan Y, Palanisamy CP, Jayaraman S, Natarajan PM, Umapathy VR, Gopathy S, Roy JR, Sadagopan JC, Thalamati D, Mironescu M. Materials-based drug delivery approaches: Recent advances and future perspectives. Green Processing and Synthesis. 2024; 13: 20230094.
26. Umapathy V, Dhanavel A, Kesavan R, Natarajan PM, Bhuminathan S, Vijayalakshmi P. Anticancer Potential of the Principal Constituent of Piper nigrum, Piperine: A Comprehensive Review. Cureus. 2024; 16(2): e54425.
27. Natarajan PM, Bhuminathan S, Rajan R, Bindu K, Loganathan K, Veerakumar R. The Crucial Role of Smoking Cessation in Preventing Oral Cancer. Journal of Pharmacy and Bioallied Sciences. 2024; 16(5): S4245-S4247.
28. Umapathy VR, Swamikannu B, Natarajan PM, Devi R, Nandini MS, Vimalarani, Vijayalakshmi P. In Silico Molecular Docking of Ocimum sanctum Phytochemicals: Targeting Key Biomarkers in Oral Cancer. Journal of Pharmacy and Bioallied Sciences. 2024; 16(5): S4792-S4799.
29. Natarajan PM, Umapathy VR. Role of transcriptomics in the study of oral cancer. Frontiers in Oral Health. 2025; 6:1524364.

30. Swamikannu B, Umapathy VR, Natarajan PM, Nandini MS, Stylin AGSQ, Vimalarani V, Rajinikanth S. Unlocking the Therapeutic Benefits of Artemisia Annua: A Comprehensive Overview of its Medicinal Properties. Journal of Pharmacy and Bioallied Sciences. 2024; 16(5): S4248-S4253.
31. Huang Y, Guo H, Liu Y, Jin W, Palanisamy CP, Pei J, Oz F, El-Aty AMA. Effects of Natural Polysaccharides on the Gut Microbiota Related to Human Metabolic Health. Molecular Nutrition & Food Research. 2025; 69:e202400792.
32. Poornima K, Meenakshi K.C, Manikandan V.R, Shankari G, Prabhu D, Rathi M.A, Palanisamy CP, Balaji R, Gopalakrishnan V.K. Exploring the anticancer potential of Jerantinine A from Tabernaemontana coronaria against prostate, breast, and ovarian cancers: A computational approach. Journal of Complementary and Integrative Medicine, 2025 22(2): 363–372.
33. Palanisamy CP, Poompradub S, Sansanaphongpricha K, Jayaraman S, Subramani K. Faridah Sonsudin gGreen synthesis of Nigella sativa-mediated silver nanoparticles for enhanced antibacterial activity and wound healing: Mechanistic insights and biomedical applications. Environmental Nanotechnology, Monitoring & Management. 2025; 24: 101085.
34. Surendran N, Raju MV, Chandrasekaran MK, Ahalliya RM, Palanisamy CP, Chandrasekaran G, Kanniappan GV. Physicochemical characterization of starch from Maranta arundinacea L.(arrowroot) rhizomes and its inhibition of COX-2: In vivo validation. Bioactive Carbohydrates and Dietary Fibre. 2025; 33: 100465.
35. Kannappan P, Chandrasekaran MK, Raju MV, Gopalakrishnan S, Dhamodharan P, Ahalliya RM, Palanisamy CP, Raju B, Kanniappan GV. Exploring the anticancer potential of Jerantinine A from Tabernaemontana coronaria against prostate, breast, and ovarian cancers: a computational approach. Journal of Complementary and Integrative Medicine. 2025; 22(02): 363-372.
36. Pei J, Kumarasamy RV, Jayaraman S, Kanniappan GV, Long Q, Palanisamy CP. Quercetin-functionalized nanomaterials: Innovative therapeutic avenues for Alzheimer's disease management. Ageing Research Reviews. 2025; 104: 102665.
37. Jayaraman S, Prasad M, Natarajan SR, Krishnamoorthy R, Alshuniaber MA, Gatasheh MK, Veeraraghavan VP, Rajagopal P, Palanisamy CP. Molecular mechanisms underlying the effects of beta-sitosterol on TGF-β1/Nrf2/SIRT1/p53-mediated signaling in the kidney of a high-fat diet and sucrose-induced type-2 diabetic rat. Chemico-Biological Interactions. 2025; 411: 111443.
38. Huang Y, Guo H, Liu Y, Jin W, Palanisamy CP, Pei J, Oz F, El-Aty AMA. Effects of Natural Polysaccharides on the Gut Microbiota Related to Human Metabolic Health. Molecular Nutrition & Food Research. 2025; e202400792.
39. Prabhakaran P, Palanisamy CP, Shanmugam A, Damodharan P, Swaminathan H, Devaraj D, Ahalliya RM, Kanniappan GV. Isolation, structural characterization, and molecular docking studies on the bioactive compound from n-Hexane extract of Emilia sonchifolia (L.) DC against the pancreatic cancer target Aurora 2 Kinase. Journal of Complementary and Integrative Medicine. 2024; 22(1): 0290.
40. Jiang H, Kumarasamy RV, Pei J, Raju K, Kanniappan GV, Palanisamy CP. Integrating engineered nanomaterials with extracellular vesicles: Advancing targeted drug delivery and biomedical applications. Frontiers in Nanotechnology. 2024; 6: 1513683.
41. Ganesan A, Kumar NG, Natarajan PM. Solanum trilobatum leaf extract-derived silver nanoparticles downregulate the PI3K/AKT/mTOR signaling pathway and attenuate oral squamous cell carcinoma cell proliferation. Journal of Herbmed Pharmacology. 2024; 13(2): 300-307.
42. Perumal MKK, Renuka RR, Subbiah SK, Natarajan PM. Artificial intelligence-driven clinical decision support systems for early detection and precision therapy in oral cancer: a mini review. Frontiers in Oral Health. 2025; 6: 1592428.
43. Ramesh E, Ganesan A, Lakshmi KC, Natarajan PM. Artificial intelligence-based diagnosis of oral leukoplakia using deep convolutional neural networks Xception and MobileNet-v2. Frontiers in Oral Health. 2025; 6: 1414524.
44. Natarajan PM. Computational Studies on Recent Congeners of Fluoroquinolones and Nitroimidazoles for Their Use in Periodontal Therapy. Journal of Pharmacy and Bioallied Sciences. 2024; 16(5): S4731-S4740.
45. Ganesan A, Kumar NG, Natarajan PM. Anticancer activity of silver nanoparticles synthesized from aqueous leaf extract of Solanum trilobatum (Purple fruit pea eggplant) on human oral cancer cells. Journal of Herbmed Pharmacololgy. 2024; 13(2): 260-268.
46. Kunamalla R, Panagal M, Palanisamy CP. Biogenic synthesis and fabrication of starch/PVA/CuO electrospun nanoscaffolds from Sargassum ilicifolium (brown marine macroalgae) extract for anticancer activity on HT-29 and MCF-7 cancer cells. Biocatalysis and Agricultural Biotechnology. 2026; 72: 103923.
47. Pei J, Govindaraj H, Sivaramakrishnan R, Kanniappan GV, Pandurangan V, Dhayalan VK, Mironescu M, Mironescu ID, Jayaraman S, Palanisamy PC. Sustainable fabrication of biopolymer-based (starch/PVA) nanoscaffolds loaded with green-synthesized CuO nanoparticles from Sargassum wightii (marine macroalgae): Cytocompatibility and antioxidant activity. Biomaterials Advances. 2026; 182: 214660.
48. Pei J, Perumal NC, Meng P, Long Q, Palanisamy CP. Extracellular vesicle-based biosensors for Alzheimer's disease: A new frontier in precision diagnostics. Ageing Research Reviews. 2026; 113: 102904.
49. Shree P, Sivaramakrishnan R, Kanniappan GV, Pandurangan V, Jayaraman S, Dhayalan VK, Mironescu M, Mironescu ID, Palanisamy CP. Antioxidant and biocompatible CuO-starch/PVA nanoscaffolds via ultrasonic green synthesis using Turbinaria conoides (brown marine macroalgae). Medicine in Drug Discovery. 2025; 28: 100238.
50. Gong J, Lin J, Guan T, Pei J, Palanisamy CP, El-AtyFrom AMA. selenium tolerance to nanoplastic antagonism: Comprehensive characterization of L. casei SNUT1 and its extracellular vesicle–nanoselenium complex. Food Bioscience. 2025; 74: 107749.

51. Poochi SP, Sundarraj R, Raju MV, Chandrasekaran MK, Ahalliya RM, Palanisamy CP, Kanniappan GV, Kondapavuluri BK, Thiruvengadam M. Harnessing Nature: Computational and Experimental Insights Into Ipomoea obscura Metabolites for Bladder Cancer Therapy. Chemistry and Biodiversity. 2025; 0: e00909.
52. Dugganaboyana GK, Kannankumar MKG, Shivaramakrishna S, Raju MV, Chandrasekaran MK, Ahalliya RM, Panneerselvam N, Palanisamy CP, Kanniappan GV. Phytochemical insights, antioxidant activity and therapeutic potential of Cassia senna against prostate cancer in Wistar albino rats. Discover Applied Sciences. 2025; 7:1206.
53. Natarajan SR, Krishnamoorthy R, Alshuniaber MA, Gatasheh MK, Rajagopal P, Veeraraghavan VP, Palanisamy CP, Jayaraman S. KDM1A Facilitates Oncogenic Potential in Colorectal Cancer Progression Through the Activation of AXIN/GSK3β/β-Catenin Signaling Pathways: Evidence From Integrated Transcriptomics and In Vitro Studies. The Journal of Gene Medicine. 2025; 27(11): e70053.
54. Guan T, Gong J, Lin J, Palanisamy CP, Jinjin Pei J, El-Aty AMA. Machine learning-driven multimodal optimization of selenium biotransformation and flavor profiling in fermented apple–Yacon functional beverages. Innovative Food Science & Emerging Technologies. 2025; 105: 104198.
55. Natarajan SR, Krishnamoorthy R, Alshuniaber MA, Alsulami TS, Gatasheh MK, Rajagopal P, Palanisamy CP, Govindan R, Veeraraghavan VP, Jayaraman S. ABCE1 facilitates tumour progression via aerobic glycolysis and inhibits cell death in human colorectal cancer cells through the p53 signalling pathway. Scientific Reports. 2025; 15: 24674.
56. Natarajan PM. Dental Bioinformnatics-Current Scope and Future perspectives. Research Journal of Pharmacy and Technology. 2022;15(5):2351-6.
57. Vidhyarekha U, Natarajan PM, Bhuminathan S, Sabarinathan J, Suba R, Vijayalakshmi P. Role of artificial intelligence in Oral Cancer. Advances in Public Health. 2024. 2024: 3664408.
58. Ganesan A, Kumar NG, Natarajan PM, Gauthaman J. Automated classification of elongated styloid processes using deep learning models-an artificial intelligence diagnostics. Frontiers in Oral Health. 2025; 5: 1424840.
59. Umapathy VR, Natarajan PM, Swamikannu B. Regenerative Strategies in Dentistry: Harnessing Stem Cells, Biomaterials and Bioactive Materials for Tissue Repair. Biomolecules. 2025; 15: 546.
60. Natarajan PM, Umapathy VR, Murali A, Swamikannu B. (2022). Computational Simulations of Identified marine-derived Natural Bioactive Compounds As Potential Inhibitors of Oral Cancer. Future Science OA. 2022; 8(3).
61. Surendran N, Chandrasekaran G, Raju MV, Chandrasekaran MK, Ahalliya RM, Palanisamy CP, Kanniappan GV, Arcot R, Alharbi NS, Thiruvengadam M. Anti-inflammatory potential of ethanolic extract of Maranta arundinacea L.: Insights from COX-2 modulation and oxidative stress analysis. South African Journal of Botany. 2026; 195: 142-151.
62. Pei J, Senthilkumar MV, Hessini K, Subramaniyam S, Sivaramakrishnan R, Kanniappan GV, Jayaraman S, Palanisamy CP. Green fabrication of starch/PVA/CuO nanoscaffolds using marine macroalgae extract for enhanced anti-inflammatory activity. Sustainable Chemistry and Pharmacy. 2026; 51: 102397.
63. Balasubramanian V, Loganathan L, Muthuswamy K, Viswanathan TM, Raju MV, Chandrasekaran MK, Ahalliya RM, Poorasamy J, Palanisamy CP, Dominic S, Kanniappan GV. Anticancer therapeutic efficacy of PEGylated β-galactosidase from Aspergillus terreus in DMBA-induced breast cancer: Toxicological, molecular and histopathological evaluation in Wistar rats. International Journal of Biological Macromolecules. 2026; 360: 151856.
64. Jayaraman S, Eswaran A, Rajagopal P, Palanisamy CP, Veerakumar P, Veeraraghavan VP, Sirasanagandla SR. Neuroendocrine-associated epigenetic factors in cellular senescence: mechanisms and therapeutic implications. Biogerontology. 2026; 27(2): 64.
65. Ponnusamy B, Rajagopal P, Palanisamy CP, Veeraraghavan VP, Jayaraman S. Mechanistic Exploration of the anticancer activity of Justicia adhatoda Plant Leaf Ethanolic Extract against Colon Cancer Cells: An in silico and in vitro Approach. Asian Pacific Journal of Cancer Prevention. 2026; 27(3): 1069-1080.
66. Pei J, Saran VS, Sivaramakrishnan R, Kanniappan GV, Pandurangan V, Jayaraman S, Dhayalan VK, Mironescu M, Mironescu ID, Palanisamy CP. Ultrasonic-assisted, Sargassum ilicifolium (brown marine macroalgae)-mediated biogenic synthesis of CuO nanoparticles incorporated in starch/PVA electrospun nanoscaffolds: In vitro safety and antioxidant efficacy assessment. Bioorganic Chemistry. 2026; 173: 109679.
67. Raj MAPA, Subramaniyam S, Kanniappan GV, Jayaraman S, Palanisamy CP. Sustainable fabrication of starch/PVA/CuO electrospun nanoscaffolds from Turbinaria ornata (marine macroalgae) extract: Physicochemical characterization and antidiabetic evaluation. Kuwait Journal of Science. 2026; 53(2): 100545.
68. Pei J, Ganesh NS, Subramaniyam S, Sivaramakrishnan R, Kanniappan GV, Jayaraman S, Palanisamy CP. Sustainable fabrication of starch/PVA/CuO electrospun nanoscaffolds from Padina tetrastromatica (Brown macroalgae) extract: Physicochemical characterization and antidiabetic assessment. Sustainable Chemistry One World. 2026; 9: 100195.
69. Sakthiraj A, Sivaramakrishnan R, Subramaniyam S, Kanniappan GV, Pandurangan V, Jayaraman S, Dhayalan VK, Mironescu M, Mironescu ID, Palanisamy CP. Chemical Physics Impact. Starch/PVA electrospun nanoscaffolds loaded with ultrasonic-assisted green-synthesis of CuO nanoparticles from marine macroalgae (Gracilaria corticata) extract: Cytotoxicity and antioxidant analysis. 2026; 12: 101018.
70. Raju M, Chandrasekaran MK, Loganathan L, Ahalliya RM, Mironescu M, Mironescu ID, Palanisamy CP, Kanniappan GV. Lipid remodeling and ferroptosis in phosphatidylcholine-mediated tumor–stroma crosstalk. Frontiers in Molecular Biosciences. 2026; 13: 1742305.
71. Rokunuzzaman MK. The Nanotech Revolution: Advancements in Materials and Medical Science. Journal of Advancements in Material Engineering. 2024:1-10.
72. Jabeen S, Veg E, Ahmad MI, Bala S, Khan T. A Comprehensive Review on Metal Oxide-based Nanomaterials: Synthesis, Characterization, Environmental, and Therapeutic Applications. ChemistrySelect. 2025;10(11):e202500080.

73. Devaraji M, Thanikachalam PV, Elumalai K. The potential of copper oxide nanoparticles in nanomedicine: a comprehensive review. Biotechnology notes. 2024.
74. Kirubakaran D, Wahid JBA, Karmegam N, Jeevika R, Sellapillai L, Rajkumar M, et al. A comprehensive review on the green synthesis of nanoparticles: advancements in biomedical and environmental applications. Biomedical Materials & Devices. 2025:1-26.
75. Khan F, Shahid A, Zhu H, Wang N, Javed MR, Ahmad N, et al. Prospects of algae-based green synthesis of nanoparticles for environmental applications. Chemosphere. 2022;293:133571.
76. Villagrán Z, Anaya-Esparza LM, Velázquez-Carriles CA, Silva-Jara JM, Ruvalcaba-Gómez JM, Aurora-Vigo EF, et al. Plant-based extracts as reducing, capping, and stabilizing agents for the green synthesis of inorganic nanoparticles. Resources. 2024;13(6):70.